

High Impact Publications with the HALO AI Deep Learning Classifier Add-On

HALO AI, the Deep Learning Classifier Add-on to the HALO® image analysis platform continues to advance research areas as diverse as infectious disease, metabolism, gastric pathology, neuroscience, myology, and oncology and immuno-oncology. Here we list recent HALO AI publications according to research area and highlight which HALO AI network was used.

Although many publications could have been placed into several categories, they are only listed once. Check any related categories for additional publications in your research area.

Infectious Disease

Pulmonary *Mycobacterium tuberculosis* control associates with CXCR3- and CCR6-expressing antigen-specific Th1 and Th17 cell recruitment

Authors: Shanmugasundaram U, Bucsan A, Ganatra S, Ibegbu C, Quezada M, Blair R, Alvarez X, Velu V, Kaushal D, Rengarajan J

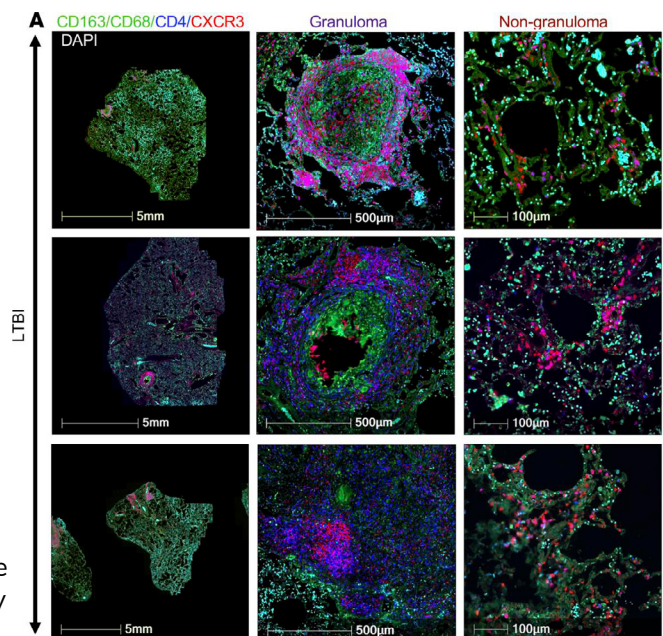
Source: <https://insight.jci.org/articles/view/137858>

Modification: Cropped

License: CCBY 4.0, <http://creativecommons.org/licenses/by/4.0/>

Science: While only a minority of individuals develop active tuberculosis (TB) after being in contact with someone with active TB, most people successfully control the infection and are asymptomatic. This is known as latent tuberculosis infection (LTBI) and a range of clinical outcomes are associated with this state. Therefore, understanding the mechanisms of immune control may provide insight into understanding how active TB is prevented. Researchers set out to better understand the role of T cells in LTBI and used a rhesus macaque model to study antigen-specific T cells in lung compartments infected with *M. tuberculosis* by sampling bronchoalveolar lavage and blood samples post infection. They identified more memory CD4+ and CD8+ T cells producing IFN- γ in the airways compared to blood and most of the *M. tuberculosis* specific CD4+ cells expressed CXCR3 and CCR6. They found that CXCR3+ CD4+ cells were found in granulomatous and nongranulomatous regions of the lung and were inversely correlated with *M. tuberculosis* burden.

Technology: The HALO [Tissue Classifier Add-on](#) was used to identify tissue on slides and output annotations. The annotations were then analysed by the VGG network of HALO AI to identify granulomas. Results were confirmed by a board-certified veterinary pathologist and the percentage of granuloma area was calculated by dividing the granuloma area by the area of the annotated region. In the image above, CD163, CD68, CD4, and CXCR3 are shown in representative LTBI cases and granulomatous and non-granulomatous areas of lung tissue.



Infectious Disease

Aid M, Vidal S, Piedra-Mora C et al. Ad26.COV2.S prevents upregulation of SARS-CoV-2 induced pathways of inflammation and thrombosis in hamsters and rhesus macaques. *Plos Pathog* **18(4)**: e1009990 (2022). DOI: [10.1371/journal.ppat.1009990](https://doi.org/10.1371/journal.ppat.1009990)

Fears A, Beddingfield B, Chirichella N et al. Myeloid cell-driven nonregenerative pulmonary scarring is conserved in multiple nonhuman primate species regardless of SARS-CoV-2 infection modality. *bioRxiv* **11(28)**: 470250 (2021). DOI: [10.1101/2021.11.28.470250](https://doi.org/10.1101/2021.11.28.470250)

Han K, Blair R, Iwanaga N et al. Lung Expression of Human Angiotensin-Converting Enzyme 2 Sensitizes the Mouse to SARS-CoV-2 Infection. *Am J Resp Cell Mol Biol* **64(1)**: 79-88 (2020). DOI: [10.1165/rcmb.2020-0354OC](https://doi.org/10.1165/rcmb.2020-0354OC)

Iwanaga N, Cooper L, Rong L et al. ACE2-IgG1 fusions with improved in vitro and in vivo activity against SARS-CoV-2. *iScience* **25(1)**: 103670 (2022). DOI: [10.1016/j.isci.2021.103670](https://doi.org/10.1016/j.isci.2021.103670)

Nienhold R, Ciani Y, Koelzer VH et al. Two distinct immunopathological profiles in autopsy lungs of COVID-19. *Nat Commun* **11**: 5086 (2020). DOI: [10.1038/s41467-020-18854-2](https://doi.org/10.1038/s41467-020-18854-2)

Okoye A, Duell D, Fukazawa Y et al. CD8+ T cells fail to limit SIV reactivation following ART withdrawal until after viral amplification. *J Clin Invest* **131(8)**: e141677 (2021). DOI: [10.1172/JCI141677](https://doi.org/10.1172/JCI141677)

Zaizen Y, Kanahori Y, Ishijima S et al. Deep-Learning-Aided Detection of Mycobacteria in Pathology Specimens Increases the Sensitivity in Early Diagnosis of Pulmonary Tuberculosis Compared with Bacteriology Tests. *Diagnostics* **12(3)**: 709 (2022). DOI: [10.3390/diagnostics12030709](https://doi.org/10.3390/diagnostics12030709)

Gastric Pathology

Abrams, J, Del Portillo A, Hills C et al. Randomized Controlled Trial of the Gastrin/CCK2 Receptor Antagonist Netazepide in Patients with Barrett's Esophagus. *Can Prev Res* **14(6)**: 675-682 (2021). DOI: [10.1158/1940-6207.CAPR-21-0050](https://doi.org/10.1158/1940-6207.CAPR-21-0050)

Franklin M, Schultz F, Tafoya M et al. A Deep Learning Convolutional Neural Network Can Differentiate Between *Helicobacter Pylori* Gastritis and Autoimmune Gastritis With Results Comparable to Gastrointestinal Pathologists. *Arch Pathol Lab Med* **146(1)**: 117-122 (2021). DOI: [10.5858/arpa.2020-0520-OA](https://doi.org/10.5858/arpa.2020-0520-OA)

Martin D, Hanson J, Gullapalli R et al. A Deep Learning Convolutional Neural Network Can Recognize Common Patterns of Injury in Gastric Pathology. *Arch Pathol Lab Med* **144(3)**: 370-378 (2019). DOI: [10.5858/arpa.2019-0004-OA](https://doi.org/10.5858/arpa.2019-0004-OA)

Metabolism

de Almeida-Faria J, Duque-Guimarães D, Ong T et al. Maternal obesity during pregnancy leads to adipose tissue ER stress in mice via miR-126-mediated reduction in Lunapark. *Diabetologia* **64**: 890-902 (2021). DOI: [10.1007/s00125-020-05357-4](https://doi.org/10.1007/s00125-020-05357-4)

Hammerle C, Sandovici I, Brierley et al. Mesenchyme-derived IGF2 is a major paracrine regulator of pancreatic growth and function. *PLoS Genet* **16(10)**: e1009069 (2020). DOI: [10.1371/journal.pgen.1009069](https://doi.org/10.1371/journal.pgen.1009069)

Petkevicius K, Virtue S, Bidault G et al. Accelerated phosphatidylcholine turnover in macrophages promotes adipose tissue inflammation in obesity. *Elife* **8**: e47990 (2019). DOI: [10.7554/eLife.47990](https://doi.org/10.7554/eLife.47990)

Myology

Kitsuka T, Shiraki A, Oyama J et al. A novel soluble epoxide hydrolase vaccine protects murine cardiac muscle against myocardial infarction. *Sci Rep* **12**: 6923 (2022). DOI: [10.1038/s41598-022-10641-x](https://doi.org/10.1038/s41598-022-10641-x)

Tau isoforms are differentially expressed across the hippocampus in chronic traumatic encephalopathy and Alzheimer's disease

Authors: Cherry J, Esnault C, Baucom Z, Tripodis Y, Huber B, Alvarez V, Stein T, Dickson D, McKee A

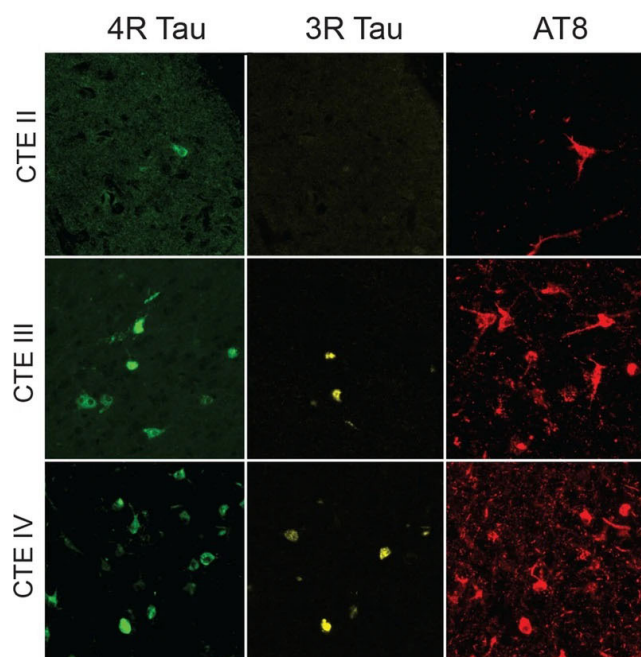
Source: <https://doi.org/10.1186/s40478-021-01189-4>

Modification: Cropped

License: CCBY 4.0, <http://creativecommons.org/licenses/by/4.0/>

Science: Alzheimer's disease (AD) and chronic traumatic encephalopathy (CTE) are both neurodegenerative diseases characterized by depositions of the tau protein. Jonathan Cherry and colleagues set out to understand how these two diseases impact the hippocampus by investigating the localization and abundance of the 3R and 4R tau isoforms. In CTE, they found a higher abundance of tau in the CA2 and CA3 subfields of the hippocampus, as compared to CA1. In AD, they found the opposite result. In both CTE and AD they found that early-stage disease was characterized by higher levels of the 4R isoform while later stage disease had more 3R. This study advances our understanding of tauopathies and provides a mechanism to differentiate CTE from AD.

Technology: Biomarkers including 3R Tau, 4R Tau, and AT8 were selected for an immunofluorescence study using the Vectra Polaris™ system from Akoya Bioscience to analyse tissue from the posterior hippocampus. Following spectral unmixing, images were opened in HALO and two HALO AI Nuclear Phenotyper algorithms were trained. The first recognized 3R+ AT8+ cells and the second identified 4R+ AT8+ cells. Over 500 annotations were used to train each algorithm for greater than 50,000 iterations. The HALO AI results were validated by neuropathologists. HALO AI was also used in nuclear segmentation in this experiment. In the image shown above, the 3R, 4R, and AT8 biomarkers are visualized across stages of CTE.



Morozzi G, Rothen J, Toussaint G et al. STING regulates peripheral nerve regeneration and colony stimulating factor 1 receptor (CSF1R) processing in microglia. *iScience* **24(12)**: 103434 (2021). DOI: [10.1016/j.isci.2021.103434](https://doi.org/10.1016/j.isci.2021.103434)

Oncology and Immuno-oncology

Amin R, Shukla A, Zhu J et al. Nuclear pore protein NUP210 depletion suppresses metastasis through heterochromatin-mediated disruption of tumor cell mechanical response. *Nat Commun* **12**: 7216 (2021). DOI: [10.1038/s41467-021-27451-w](https://doi.org/10.1038/s41467-021-27451-w)

Basu S, Luke B, Karim B et al. CK2 signaling from TOLLIP-dependent perinuclear endosomes is an essential feature of KRAS mutant cancers. *bioRxiv* (2022). DOI: [10.1101/2022.04.05.487175](https://doi.org/10.1101/2022.04.05.487175)

De Logu F, Monteiro de Araujo D, Ugolini F et al. The TRPA1 Channel Amplifies the Oxidative Stress Signal in Melanoma. *Cells* **10(11)**: 3131 (2021). DOI: [10.3390/cells10113131](https://doi.org/10.3390/cells10113131)

Esce A, Redemann J, Sanchez A et al. Predicting nodal metastases in papillary thyroid carcinoma using artificial intelligence. *Am J Surg* **222(5)**: 952-958 (2021). DOI: [10.1016/j.amjsurg.2021.05.002](https://doi.org/10.1016/j.amjsurg.2021.05.002)

Establishing standardized immune phenotyping of metastatic melanoma by digital pathology

Authors: Sobottka B, Nowak M, Frei AL, Haberecker M, Merki S, Tumor Profiler consortium, Levesque MP, Dummer R, Moch H, Koelzer VH

Source: <https://www.nature.com/articles/s41374-021-00653-y>

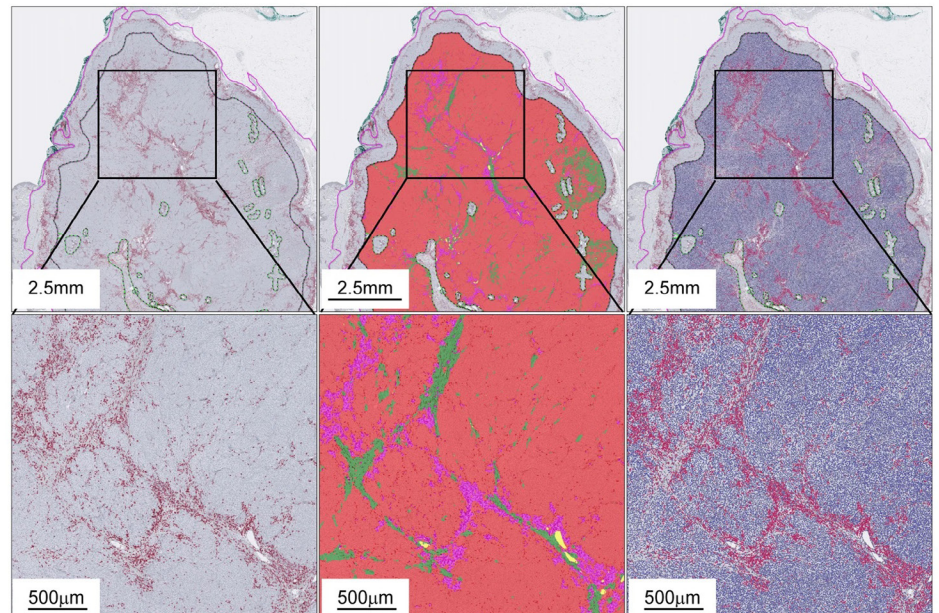
Modification: Cropped

License: CC BY 4.0, <http://creativecommons.org/licenses/by/4.0/>

Science: CD8+ tumor-infiltrating T cells are increasingly acknowledged as an important predictive biomarker for immunotherapy stratification in malignant melanoma. Nevertheless, it is difficult to achieve a quantitative and reproducible approach to

examining their prevalence within tumors, and it has remained challenging to translate these results into clinically actionable immune phenotypes. As part of the Tumor Profiler Study, researchers at the University Hospital Zürich led by Dr. Bettina Sobottka and Prof. Viktor Koelzer developed a computational diagnostic algorithm prototype using HALO and HALO AI to a) quantitatively measure spatial densities of tumor-infiltrating CD8+ T cells as the key anti-tumoral effector population b) localize the immune cell infiltrates to specific microenvironment compartments and c) derive spatially resolved infiltration maps in metastatic melanoma implemented on a standardized, clinical grade platform. This approach thus efficiently classifies metastatic melanoma into the clinically relevant immune diagnostic categories “inflamed”, “excluded” and “desert” and has great potential for clinical translation.

Technology: The DenseNet deep learning network of HALO AI was trained on pathologist-defined annotations to differentiate the following tissue classes: cancer tissue, desmoplastic stroma, immune-infiltrated stroma, glass, pigment deposition, as well as haemorrhage and necrosis. Classifier training was an iterative process where expert pathologists reviewed classifier mark-up results and provided corrections. Performance of the final classifier was tested on images and annotations not included in the training and validation dataset. In the image shown above, the left panels show the IHC, the middle panels show the HALO AI classifier mark-up image, and the right panels show the cell segmentation and markup in HALO.



Guo, L, Cao, C, Goswami S et al. Tumoral PD-1hi CD8+ T cells are partially exhausted and predict favorable outcome in triple-negative breast cancer. *Clin Sci* **134**(7): 711-726 (2020). DOI: [10.1042/CS20191261](https://doi.org/10.1042/CS20191261)

Horeweg N, Bruyn M, Nout R et al. Prognostic Integrated Image-Based Immune and Molecular Profiling in Early-Stage Endometrial Cancer. *Cancer Immunol Res* **8**(12): 1508-1519 (2020). DOI: [10.1158/2326-6066.CIR-20-0149](https://doi.org/10.1158/2326-6066.CIR-20-0149)

Horeweg N, Workel H, Loiero D et al. Tertiary lymphoid structures critical for prognosis in endometrial cancer patients. *Nat Commun* **13**: 1373 (2022). DOI: [10.1038/s41467-022-29040-x](https://doi.org/10.1038/s41467-022-29040-x)

Hvid H, Skydsgaard M, Jensen N et al. Artificial Intelligence-Based Quantification of Epithelial Proliferation in Mammary Glands of Rats and Oviducts of Göttingen Minipigs. *Toxicol Pathol* **49**(4): 912-927 (2020). DOI: [10.1177/0192623320950633](https://doi.org/10.1177/0192623320950633)

Oncology and Immuno-oncology

Ilié M, Benzaquen J, Tournaire P et al. Deep Learning Facilitates Distinguishing Histologic Subtypes of Pulmonary Neuroendocrine Tumors on Whole-Slide Images. *Cancers* **14**(7): 1740 (2022). DOI: [10.3390/cancers14071740](https://doi.org/10.3390/cancers14071740)

Koelzer V, Herzig P, Zlobec I et al. Integrated functional and spatial profiling of tumour immune responses induced by immunotherapy: the iPROFILER platform. *Immunooncol Technol* **10**:100034 (2021). DOI: [10.1016/j.iotech.2021.100034](https://doi.org/10.1016/j.iotech.2021.100034)

Madueke I, Hu W, Hu D et al. The role of WNT10B in normal prostate gland development and prostate cancer. *The Prostate* **79**(14): 1692-1704 (2019). DOI: [10.1002/pros.23894](https://doi.org/10.1002/pros.23894)

Nearchou I, Ueno H, Kajiwaru Y et al. Automated Detection and Classification of Desmoplastic Reaction at the Colorectal Tumour Front Using Deep Learning. *Cancers* **13**(7): 1615 (2021). DOI: [10.3390/cancers13071615](https://doi.org/10.3390/cancers13071615)

Neeb A, Herranz N, Arce-Gallego S et al. Advanced Prostate Cancer with ATM Loss: PARP and ATR Inhibitors. *Eur Urol* **79**(2): 200-211 (2021). DOI: [10.1016/j.eururo.2020.10.029](https://doi.org/10.1016/j.eururo.2020.10.029)

Pham H, Futakuchi M, Bychkov A et al. Detection of Lung Cancer Node Metastases from Whole-Slide Histopathologic Images Using a Two-Step Deep Learning Approach. *Am J Pathol* **189**(12): 2428-2439 (2019). DOI: [10.1016/j.ajpath.2019.08.014](https://doi.org/10.1016/j.ajpath.2019.08.014)

Race AM, Sutton D, Hamm G et al. Deep Learning-Based Annotation Transfer between Molecular Imaging Modalities: An Automated Workflow for Multimodal Data Integration. *Anal Chem* **93**(6): 3061-3071 (2021). DOI: [10.1021/acs.analchem.0c02726](https://doi.org/10.1021/acs.analchem.0c02726)

Radziuviene G, Rasmusson A, Augulis R et al. Intratumoral Heterogeneity and Immune Response Indicators to Predict Overall Survival in a Retrospective Study of HER2-Borderline (IHC 2+) Breast Cancer Patients. *Front Oncol* **11**: 774088 (2021). DOI: [10.3389/fonc.2021.774088](https://doi.org/10.3389/fonc.2021.774088)

Rasmusson A, Zilenaite D, Nestarenkaite A et al. Immunogradient Indicators for Antitumor Response Assessment by Automated Tumor-Stroma Interface Zone Detection. *Am J Pathol* **190**(6): 1309-1322 (2020). DOI: [10.1016/j.ajpath.2020.01.018](https://doi.org/10.1016/j.ajpath.2020.01.018)

Redemann J, Schultz F, Martinez C et al. Comparing Deep Learning and Immunohistochemistry in Determining the Site of Origin for Well-Differentiated Neuroendocrine Tumors. *J Pathol Inform* **11**(1): 32 (2020). DOI: [10.4103/jpi.jpi_37_20](https://doi.org/10.4103/jpi.jpi_37_20)

Sakamoto T, Furukawa T, Pham H et al. Collaborative workflow between pathologists and deep learning for evaluation of tumor cellularity in lung adenocarcinoma. *bioRxiv* (2022). DOI: [10.1101/2022.01.11.475587](https://doi.org/10.1101/2022.01.11.475587)

Salotti J, Karim B, Misra S et al. 3'UTR-directed, kinase proximal mRNA decay inhibits C/EBP β phosphorylation/activation to suppress senescence in tumor cells. *bioRxiv* (2022). DOI: [10.1101/2022.03.29.486281](https://doi.org/10.1101/2022.03.29.486281)

Shiraishi T, Shinto E, Nearchou I et al. Prognostic significance of mesothelin expression in colorectal cancer disclosed by area-specific four-point tissue microarrays. *Virchows Archiv* **477**: 409-420 (2020). DOI: [10.1007/s00428-020-02775-y](https://doi.org/10.1007/s00428-020-02775-y)

Strittmatter N, Moss J, Race A et al. Multi-modal molecular imaging maps the correlation between tumor microenvironments and nanomedicine distribution. *Theranostics* **12**(5): 2162-2174 (2022). DOI: [10.7150/thno.68000](https://doi.org/10.7150/thno.68000)

Sweet S, Chain D, Yu W et al. The addition of FAIMS Increases Targeted Proteomics Sensitivity from FFPE Tumor Biopsies. *bioRxiv* (2022). DOI: [10.1101/2022.02.08.479554](https://doi.org/10.1101/2022.02.08.479554)

van Dijk N, Gil-Jimenez A, Silina K et al. The Tumor Immune Landscape and Architecture of Tertiary Lymphoid Structures in Urothelial Cancer. *Front Immunol* **12**: 793964 (2021). DOI: [10.3389/fimmu.2021.793964](https://doi.org/10.3389/fimmu.2021.793964)

Zilenaite D, Rasmusson A, Augulis R et al. Independent Prognostic Value of Intratumoral Heterogeneity and Immune Response Features by Automated Digital Immunohistochemistry Analysis in Early Hormone Receptor-Positive Breast Carcinoma. *Front Oncol* **10**(950) (2020). DOI: [10.3389/fonc.2020.00950](https://doi.org/10.3389/fonc.2020.00950)

For More Information

Visit <https://learn.indicalab.com/literature> to view all our customer publications.

To learn more about HALO AI applications including tissue segmentation, nuclear segmentation, and nuclear phenotyping, read our [HALO AI white paper](#).

Also, visit the [HALO AI webpage](#) to download application notes, eBooks, and case studies.



About Indica Labs

Indica Labs is the world's leading provider of computational pathology software and image analysis services. Our flagship [HALO®](#) and [HALO AI](#) platform facilitates quantitative evaluation of digital pathology images. [HALO Link](#) facilitates research-focused image management and collaboration while [HALO AP®](#) enables collaborative clinical case review.

Through a combination of precision, performance, scalability, and usability, our software solutions enable pharmaceutical companies, diagnostic labs, research organizations, and Indica's own [contract pharma services team](#) to advance tissue-based research, clinical trials, and diagnostics.



PHARMA SERVICES
powered by **indica labs**



Contact us for more information, demo, or trial.

US Headquarters

Indica Labs, Inc
8700 Education PI NW, Bldg B
Albuquerque, NM 87114 USA
+1 (505) 492-0979
info@indicalab.com

UK and Europe

+44 (0)1789 765 721
emea@indicalab.com

Japan

+81 (0)70 4180 7730
japan@indicalab.com

China

+86 13761896143
china@indicalab.com

Tech Support: support@indicalab.com
Website: <https://indicalab.com>



powered by **indica labs**